Springer

Journal of
Mechanical
Science and
Technology

Journal of Mechanical Science and Technology 22 (2008) 397~407

www.springerlink.com/content/1738-494x

Measurements of the flow fields around two square cylinders in a tandem arrangement

Moon Kyoung Kim[1], Dong Keon Kim[2], Soon Hyun Yoon[3] and Dae Hee Lee[4,*]

[1]*Department of Mechanical Design Chang-Won College, 196 Doodae-Dong, Changwon, Gyeongnam, Korea*
[2]*Institute of Mechanical Engineering Technology*
[3]*School of Mechanical Engineering Busan National University, Gumjung-Gu, Busan 609-735, Korea*
[4]*Inje Engineering Institute School of Mechanical and Automotive Engineering*
Inje University, 607 Obang-Dong, Gimhae, Gyeongnam 621-749, Korea

(Manuscript Received July 4, 2007; Revised October 18, 2007; Accepted October 18, 2007)

Abstract

The velocities, turbulence intensities, Reynolds shear stresses, and turbulent kinetic energies of the flow fields around two square cylinders in a tandem arrangement were investigated using particle image velocimetry (PIV). The experiments were made for the spacing between the two cylinders ranging from s/D = 0.5 to 10.0 and two Reynolds numbers of 5,300 and 16,000. The results showed that the flow patterns at s/D≤2.0 were drastically different from those at s/D≥2.5 for both Reynolds numbers. The sudden change in the flow patterns depended on the reattachment of the shear layer separated from the upstream cylinder.

Keywords: Square cylinder; Tandem arrangement; Flow fields; Critical spacing; Strouhal number; Particle image velocimetry

1. Introduction

When one structure is immersed in the wake of another, the characteristics of the flow and the aerodynamic forces depend strongly on the shape, spacing between the structures, arrangement of the structures, and wind direction. It is therefore useful to investigate these characteristics from a practical point of view. Since many high-rise buildings are affected by other nearby buildings, their design must consider the aerodynamic forces acting on the structures. It is also important to investigate the characteristics of vortex shedding caused by the flow interference of other structures since this may be connected to structural vibration problems.

Despite numerous investigations of the flow structures past circular cylinders, little attention has been directed toward the flow structures around square cylinders in a tandem arrangement. Haniu et al. [1] and Haniu and Sakamoto [2] investigated the drag force variation on two square cylinders in a tandem arrangement and determined the spacing at which a sudden increase in the drag force occurred, which is known as the critical spacing. They found that the critical spacing between two square cylinders decreased as the freestream turbulence intensity increased. Gu [3], and Gu and Sun [4] observed the aerodynamic characteristics around two circular cylinders in various arrangements, two rectangular cylinders with different aspect ratios, and groups of cooling towers at high Reynolds numbers. Hangan and Vickery [5], and Hangan et al. [6] studied complex buffeting problems of two-dimensional (2D) bluff bodies in smooth, large-scale and small-scale turbulent flows. Pressure and velocity measurements were used to complement the flow visualizations of two bluff-body buffeting configurations at similar Reynolds numbers and turbulence levels for 2D square cylinders in a free shear flow, and three-dimensional

*Corresponding author. Tel.: +82 55 320 3185, Fax.: +82 55 324 1723
E-mail address: mechdhl@inje.ac.kr
DOI 10.1007/s12206-007-1041-6

(3D) surface-mounted cubes in a thin boundary layer flow. Chen and Liu [7] showed that the flow characteristics around two square cylinders in a tandem arrangement strongly depended on the spacing and spacing variations. They observed hysteresis when the spacing was progressively increased and then decreased. Havel and Martinuzzi [8] investigated the vortex shedding from two surface-mounted cubes in a tandem arrangement within a boundary layer using phase-averaged laser Doppler velocimetry.

The existence of a critical spacing for two cylinders in a tandem arrangement at which a sudden change in the drag occurs has been reported in numerous studies [7-9]. Although the cause of the critical spacing has recently been identified by using flow visualization methods, detailed information about the flow fields around the cylinder remains scarce.

In the present study, we used particle image velocimetry (PIV) to investigate the change in the flow field as the spacing between two square cylinders in tandem arrangement was varied. Changes in the vortex shedding frequency of the upstream cylinder were also examined.

2. Experimental apparatus and methodology

2.1 Experimental conditions

A schematic diagram of the test model for the present investigation is shown in Fig. 1. Two square cylinders with 20 mm × 20 mm square cross sections and 15:1 aspect ratios were centered in line with the mean flow direction in the middle of the test section. The upstream cylinder was fixed 300 mm away from the exit of the wind tunnel. The blockage ratio was 6.6%.

The models were made of acrylic and the edges were machined as sharply as possible. Two free-stream velocities were used, 3.87 m/s and 11.68 m/s, which corresponded to Reynolds numbers of 5,300 and 16,000, respectively. The spacing between the two cylinders was varied from S/D = 0.5 to 10.0.

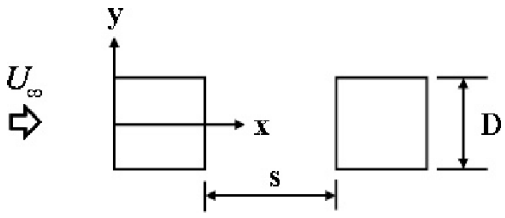

Fig. 1. Two square cylinders in a tandem arrangement.

2.2 PIV measurement system

Due to rapid advances in computers, optics, and digital image processing techniques, instantaneous velocity fields can now be extracted by particle image velocimetry (PIV), which is a reliable velocity field measurement technique [10]. The experimental setup for the single-frame PIV velocity field measurements is shown in Fig. 2. The PIV system consisted of a high-resolution CCD camera, a dual-head Nd:Yag laser, a frame grabber, a synchronizing device, and a computer. A high-resolution CCD camera with a spatial resolution of 2000 × 2000 pixels was used to capture the particle images. The maximum energy of the two-head Nd:Yag laser was 250 mJ per pulse, and the CCD camera and Nd:Yag laser were synchronized with a TSI synchronizer. For the single-frame PIV measurements, two successive particle images were recorded on a single frame.

During the first exposure of the CCD camera, the particle image scattered by the first laser pulse was recorded on the CCD sensor array. The CCD sensor array was translated by prescribed pixel lines within a time interval t, and then the second exposure started to capture the second particle image. In our experiment, the time interval between two laser pulses was set to t = 50 μs or 20 μs for Reynolds numbers of 5,300 and 16,000, respectively. The two particle images were superimposed on a single frame and the double-exposed single-frame image was then cross-correlated to extract the instantaneous velocity field. Small olive-oil droplets, 2 μm in diameter, were used as seeding tracers. These were generated from compressed air that was supplied to the olive oil through a Laskin nozzle with several fine holes.

A thin laser light sheet was formed by passing the laser beam through spherical and cylindrical lenses. The CCD camera was installed perpendicular to the laser light sheet to capture the scattered particle images of the flow. The interrogation window was 48 × 48 pixels with 50% overlap.

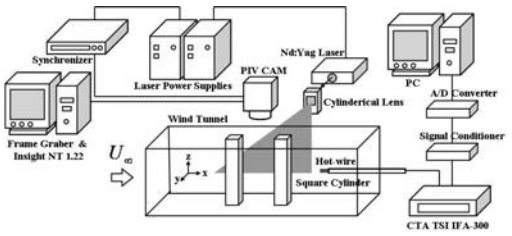

Fig. 2. Schematic diagram of the experimental setup.

To obtain the time-averaged mean flow structures, 2,000 instantaneous velocity fields were recorded for each experimental case. These instantaneous velocity fields were ensemble-averaged to obtain the spatial distributions of the mean velocity, turbulence intensity, Reynolds shear stress, and turbulent kinetic energy.

2.3 Measurement of the vortex shedding frequency

A constant-temperature anemometer (CTA, TSI IFA-300) in conjunction with a hot-wire probe was employed to detect vortex shedding from the upstream cylinder. The hot-wire probe was calibrated by a TSI-1125 velocity calibrator and a Furness FCO-510 micromanometer.

The hot-wire probe was moved by using a 3D traverse with an accuracy of 10 μm. The probe was placed at a streamwise distance of x/D = 2.5 behind the upstream cylinder in the center plane of the test section. The spanwise position of the probe was y/D = 1.0 to preclude interference in the velocity signal from vortices of the opposite sign [11-13]. The shedding frequency was determined from a power spectral density (PSD) analysis of the streamwise velocity component.

3. Results and discussion

3.1 Instantaneous velocity fields

The instantaneous spanwise velocity fields and streamlines for s/D = 2.0 and 2.5 at Reynolds numbers of 5,300 and 16,000, respectively, are shown in Figs. 3 and 4. The Reynolds number was defined by

$$\mathrm{Re} = \frac{U_\infty D}{\nu} \tag{1}$$

where U_∞ is the freestream velocity, D is the width of the square cylinder, and ν is the kinematic viscosity of the air. At Re = 5,300 and s/D = 2.0 (see Fig. 3(a)), the separated shear layer from the front edges of the upstream cylinder reattached on the lateral surface of the downstream cylinder, forming two recirculation regions between the two cylinders. This flow pattern is referred to as Mode 1. The flow reattachment of the separated shear layer on the downstream cylinder exposed the front face of that cylinder to a strong suction that created a negative drag coefficient.

When s/D = 2.5 (see Fig. 3(b)), a separated shear layer was evident between the two cylinders and the recirculation regions did not form. Thus, the downstream cylinder had a positive drag force. This flow pattern is referred to as Mode 2. These characteristics were also evident at Re = 16,000 (see Figs. 4(a) and 4(b)), although a higher spanwise velocity was broadly distributed between the two cylinders. This characteristic was observed for all instantaneous velocity fields, indicating that more fluid flowed through the gap between the two cylinders at the higher Reynolds number.

The flow patterns showed that a discontinuous jump in the drag coefficient of the both cylinders occurred simultaneously at the critical spacing, as shown in Fig. 5 [1]. This phenomenon resulted from a sudden change in the flow pattern, which depended on whether the shear layer that was separated from the upstream cylinder could reattach on the lateral face of the downstream cylinder. The critical spacing was s/D = 2.5 for both Reynolds numbers in this study. Haniu and Sakamoto [2] investigated the effect of the freestream turbulence intensity on the forces acting on two square cylinders in a tandem arrangement at $Re = 3.32 \times 10^4$. Then investigation focused on the discontinuous change in the flow pattern as the

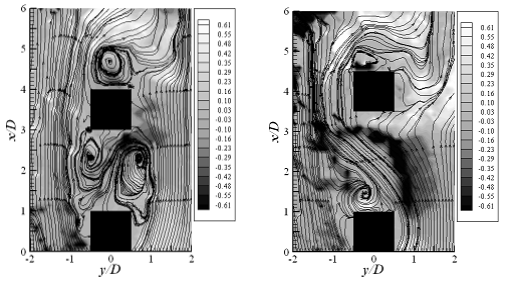

(a) s/D = 2.0 (b) s/D = 2.5

Fig. 3. Instantaneous spanwise velocity fields and streamlines at Re = 5,300.

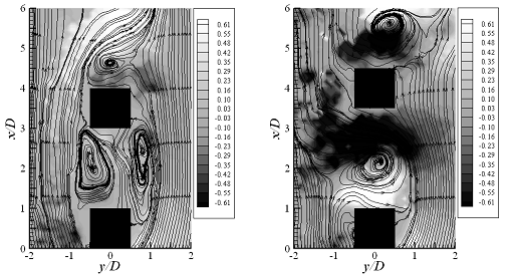

(a) s/D = 2.0 (b) s/D = 2.5

Fig. 4. Instantaneous spanwise velocity fields and streamlines at Re = 16,000.

spacing approached the critical value. The critical spacing occurred at smaller spacings as the turbulence intensity increased.

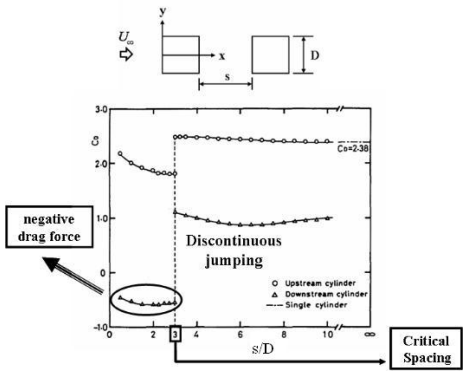

Fig. 5. Variation of the drag coefficient with the spacing (Haniu et al.,1987).

The critical spacing has also been shown to depend on the Reynolds number. The characteristics of vortex shedding from an isolated square cylinder are a strong function of the Reynolds number when $Re \leq 5300$ [14, 15]; therefore, the critical spacing decreases with the Reynolds number [7]. However, the critical spacing in the present study appeared to be unaffected by a change in the Reynolds number from 5,300 to 16,000.

3.2 Mean velocity fields

Streamlines from the ensemble-averaged velocity fields measured for s/D = 1.0~4.0 are shown in Figs. 6 and 7, respectively. Only one-half of the flow-field plane is shown due to the symmetrical flow structure along the centerline $y/D = 0$. The flow characteristics were divided into Mode 1 and Mode 2 flow

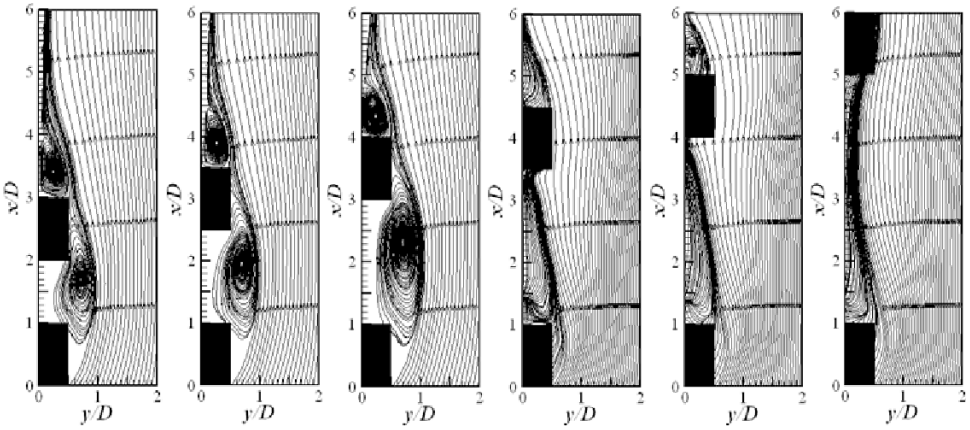

(a) s/D = 1.0 (b) s/D = 1.5 (c) s/D = 2.0 (d) s/D = 2.5 (e) s/D = 3.0 (f) s/D = 4.0

Fig. 6. Streamlines from the ensemble-averaged velocity fields at Re_D = 5300.

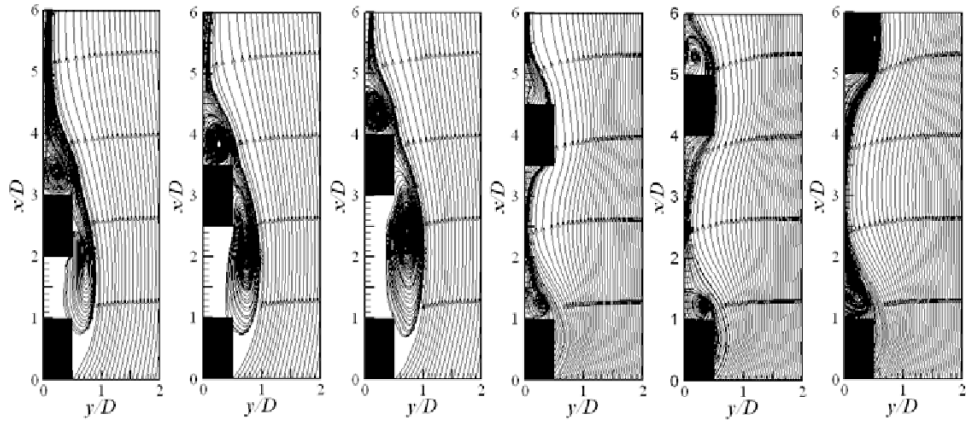

(a) s/D = 1.0 (b) s/D = 1.5 (c) s/D = 2.0 (d) s/D = 2.5 (e) s/D = 3.0 (f) s/D = 4.0

Fig. 7. Streamlines from the ensemble-averaged velocity fields at Re_D = 16000.

patterns near the critical spacing $s/D = 2.5$. The Mode 1 pattern for $s/D \leq 2.0$ had large recirculation regions between the two cylinders caused by the separated shear layer of the upstream cylinder that reattached on the lateral surface of the downstream cylinder. The Mode 2 pattern for $s/D \geq 2.5$ had separated shear layers at both the upstream and downstream cylinders.

Hangan et al. [6] obtained the mean flow streamlines at $s/D = 1.5$, shown in Fig. 8, using laser Doppler velocimetry (LDV). The upstream shear layer almost reattached on the trailing edge of the downstream cylinder and the gap vortex was deformed. The flow intermittently slipped off the trailing edge and caused bistable shedding due to overshooting and then quasi-reattaching. For smaller spacings, the flow always overshot the trailing edge, whereas for larger spacings, the shear layer rolled into the gap.

3.3 Turbulence characteristics

Contours of the mean streamwise turbulence intensity are shown in Figs. 9 and 10 for $s/D = 2.0$ and 2.5, respectively. For all flow fields, the streamwise turbulence intensity was higher for the Mode 2 flow than for the Mode 1 flow. For the Mode 2 flow, the separated shear layer had a particularly strong streamwise turbulence intensity near the downstream corners of the upstream cylinder because a separated shear layer occurred periodically at the right and left upstream corners of the upstream cylinder. A similar behavior with respect to the streamwise turbulence intensity was observed near the downstream corners of the downstream cylinder, particularly at $Re = 16{,}000$.

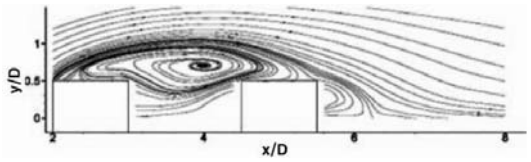

Fig. 8. Streamline representation of the LDV-measured mean velocity vectors for 2-D cylinders at $s/D = 1.5$ (Hangan et al., 1987).

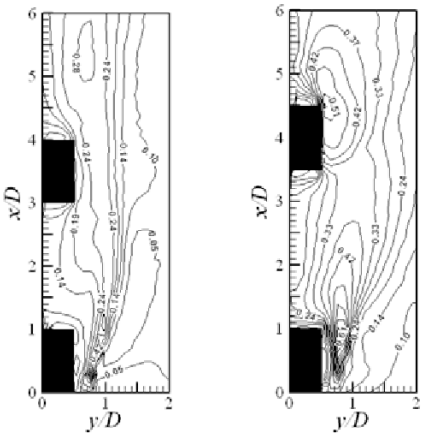

(a) $s/D = 2.0$ (b) $s/D = 2.5$

Fig. 9. Contours of the streamwise turbulence intensity at $Re = 5{,}300$.

Variations in the mean streamwise turbulence intensity measured along the centerline are shown in Fig. 11. The streamwise turbulence intensity was almost unchanged for the two Reynolds numbers.

Contours of the mean spanwise turbulence intensity are shown in Figs. 12 and 13 for $s/D = 2.0$ and $s/D = 2.5$, respectively. For the Mode 2 flow, a significant difference in the spanwise turbulence intensity between the two cylinders was observed for the two Reynolds numbers. This can be explained by the fact that the separated shear layer from the upstream cylinder extended into the gap between the two cylinders due to the higher spanwise velocity at $Re = 16{,}000$, when the strong suction behind the upstream cylinder allowed more fluid to flow around the upstream cylinder and enter the gap. The spanwise turbulence intensity was affected by the Reynolds number, despite the similar flow patterns, unlike the streamwise turbulence intensity.

Variations of the mean spanwise turbulence intensity measured along the centerline are shown in Fig. 14. For the Mode 2 flow, the turbulence intensity at $x/D = 3.0$ doubled as the Reynolds number increased from 5,300 to 16,000.

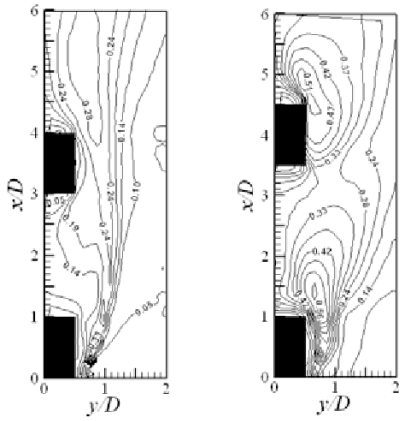

(a) $s/D = 2.0$ (b) $s/D = 2.5$

Fig. 10. Contours of the streamwise turbulence intensity at $Re = 16{,}000$.

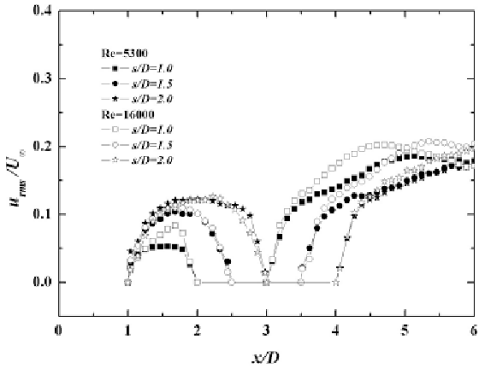

(a) Mode 1

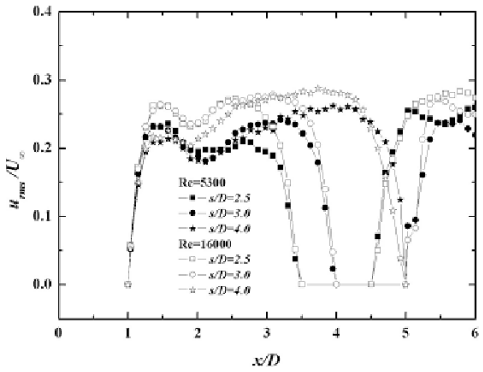

(b) Mode 2

Fig. 11. Variation in the streamwise turbulence intensity along the centerline.

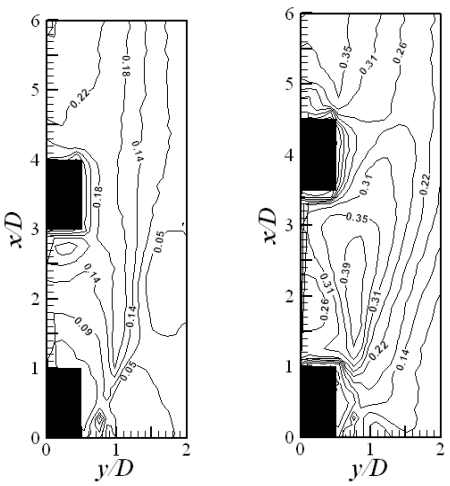

(a) s/D = 2.0 (b) s/D = 2.5

Fig. 12. Contours of the spanwise turbulence intensity at Re = 5,300.

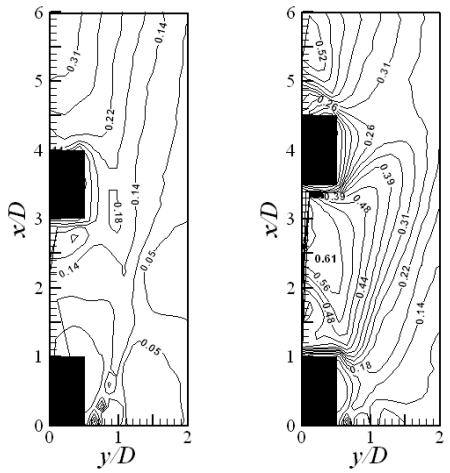

(a) s/D = 2.0 (b) s/D = 2.5

Fig. 13. Contours of the spanwise turbulence intensity at Re = 16,000.

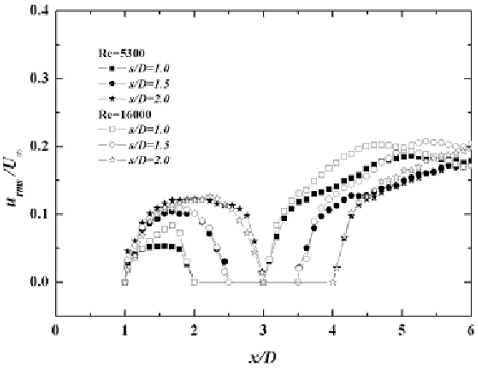

(a) Mode 1

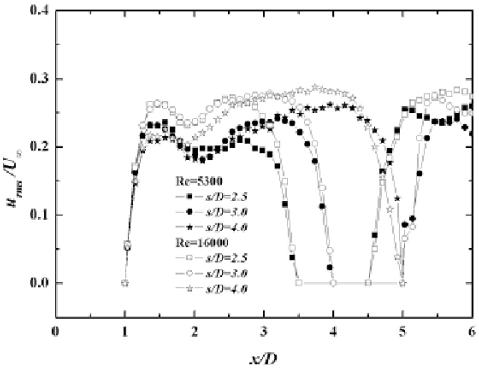

(b) Mode 2

The Reynolds number effect on 2D square cylinders in a tandem arrangement can be explained by using the Reynolds shear stress. The turbulence affects the mean velocity through the Reynolds stresses, $-\rho\overline{u_i'u_j'}$, which determines the shear flow that travels from the upstream cylinder to the gap between the two cylinders. Thus, a significant difference exists between the spanwise turbulence intensities at Re = 5,300 and Re = 16,000. The fluid motion is driven by pressure fluctuations and inertia interactions, which are large enough that viscosity is not important.

Contours of the measured Reynolds shear stress are shown in Figs. 15 and 16 for s/D = 2.0 and s/D = 2.5, respectively. In the region of x/D = 1.0–2.5 and y/D = 0.5–1.0, the distributions were greater and broader when Re was 16,000 rather than 5,300. This was attributable to a momentum difference in the transport of the separated shear flow from the upstream cylinder to the gap between the two cylinders. Thus, a significant difference existed in the spanwise turbulence intensity of the flow for the two Reynolds numbers.

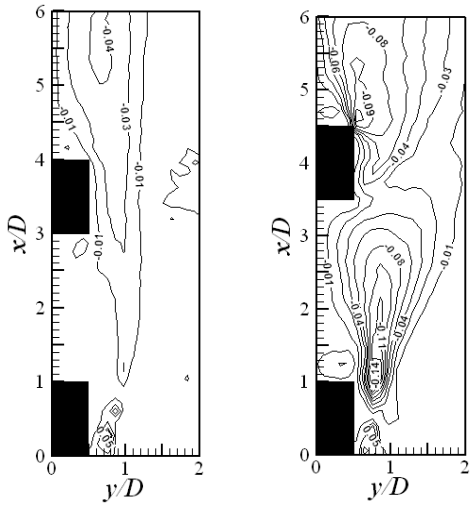

(a) s/D = 2.0 (b) s/D = 2.5

Fig. 15. Contours of the Reynolds shear stress at Re = 5,300.

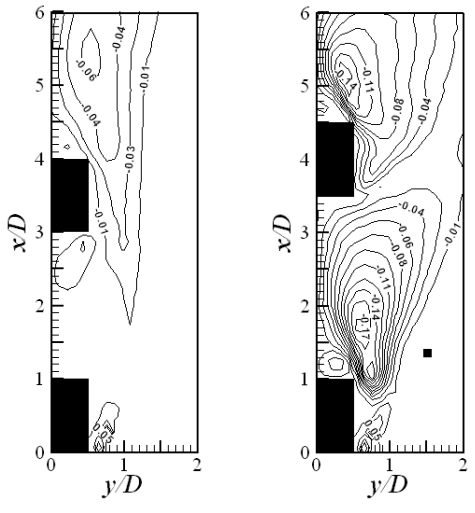

(a) s/D = 2.0 (b) s/D = 2.5

Fig. 16. Contours of the Reynolds shear stress at Re = 16,000.

The structural differences between the streamlines of the ensemble-averaged velocity fields at s/D = 2.5 for the two Reynolds numbers are shown in Fig. 17. Both flows had similar Mode 2 flow patterns with both cylinders having positive drag coefficients, and little difference between the flows was observed when the separated shear layer from the upstream cylinder entered the gap. At Re = 5,300, the separated shear layers at both upstream corners of the upstream cylinder met at the front face of the downstream cylinder.

However, at Re = 16,000, the separated shear layers met farther upstream near x/D = 2.5. If the Reynolds numbers were decreased to lower values, such as Re = 2,700, the separated shear layer would reattach on the lateral face of the downstream cylinder, as illustrated schematically in Fig. 18. Unlike a single square cylinder, for which the streamlines remain nearly unchanged with Reynolds number, the streamlines for two square cylinders in a tandem arrangement are

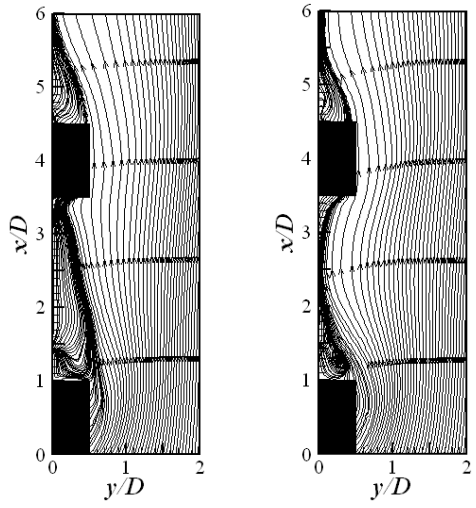

(a) Re = 5,300 (b) Re = 16,000

Fig. 17. Structural differences in the streamlines from the ensemble-averaged velocity fields at s/D = 2.5.

strongly affected by the range of Reynolds numbers examined in this study.

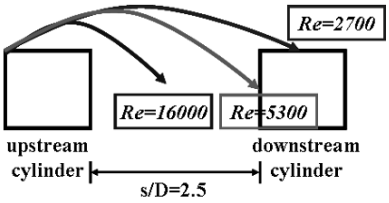

Fig. 18. Schematic diagram of the change in the streamline pattern with the Reynolds number.

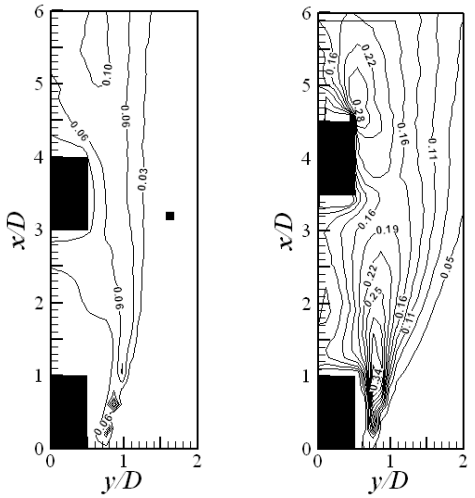

(a) s/D = 2.0 (b) s/D = 2.5

Fig. 19. Contours of the turbulent kinetic energy at Re = 5,300.

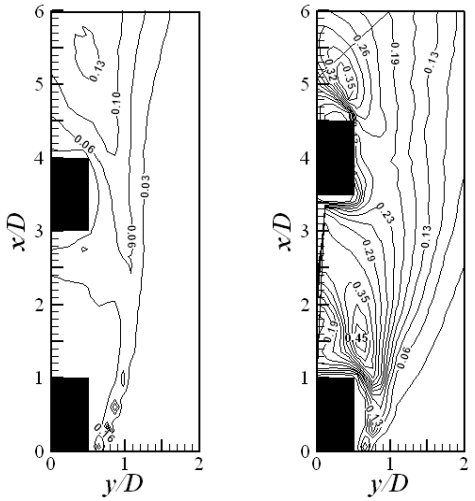

(a) s/D = 2.0 (b) s/D = 2.5

Fig. 20. Contours of the turbulent kinetic energy at Re = 16,000.

Contours of the mean turbulent kinetic energy (TKE) measured for various spacings are shown in Figs. 19 and 20. The TKE was calculated from

$$TKE = \frac{1}{2}\left(\overline{u'^2} + \overline{v'^2} + \overline{w'^2}\right) \approx \frac{3}{4}\left(\overline{u'^2} + \overline{v'^2}\right), \quad (2)$$

where the approximation $\overline{w'^2} = 0.5\left(\overline{u'^2} + \overline{v'^2}\right)$ was used because w' cannot be measured on the x-y measurement plane [16, 17]. Therefore, the true TKE will be slightly different from our results in regions in which this assumption is not valid. For the Mode 2 flow, the TKE determined by the streamwise and spanwise velocity fluctuations was also dependent on the Reynolds number.

Comparisons of the streamwise turbulence intensity with the spanwise turbulence intensity along the centerline for the Mode 2 flow are shown in Fig. 21. Because of the much larger spanwise fluctuations, the

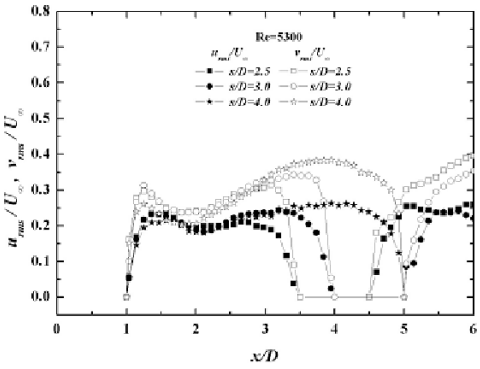

(a) Re = 5,300

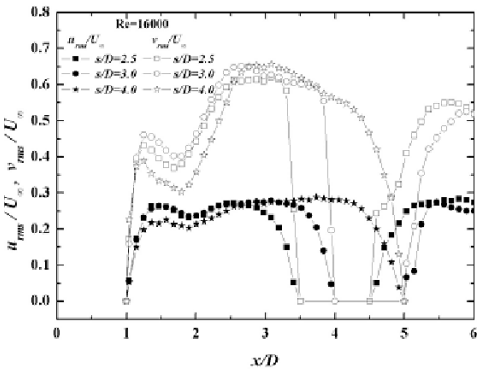

(b) Re = 16,000

Fig. 21. Comparison of the turbulence intensities along the centerline for the Mode 2 flow pattern.

TKE characteristics along the centerline, shown in Fig. 22, are similar to the spanwise turbulence intensity. For Re = 16,000, the maximum TKE observed near x/D = 0.3 was caused by the entrance of the surrounding fluids and their subsequent mixing. At the higher Reynolds number, the upstream cylinder was unaffected by the downstream cylinder, but this not the case at the lower Reynolds number.

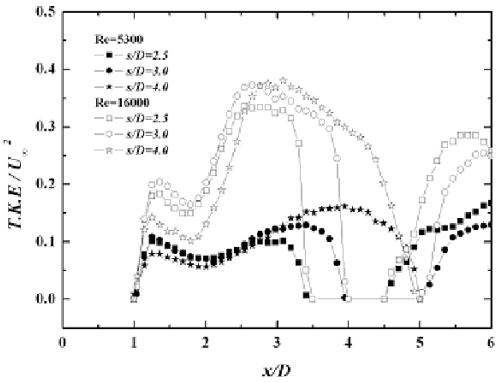

Fig. 22. Variation in the turbulent kinetic energy along the centerline for the Mode 2 flow pattern.

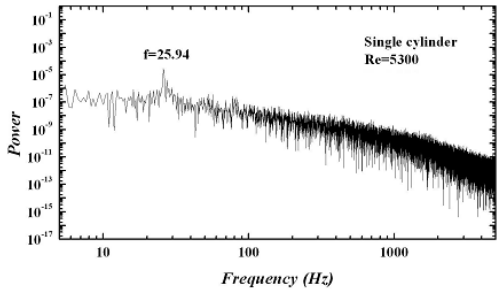

(a) Re = 5,300

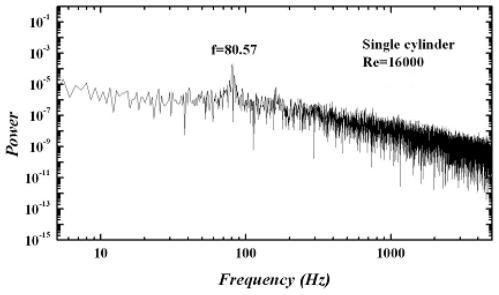

(b) Re = 16,000

Fig. 23. Power spectra of the streamwise velocity fluctuations for a single square cylinder.

3.4 Vortex shedding characteristics

A constant-temperature anemometer was used in conjunction with the hot-wire probe to investigate the effect of the spacing on the vortex shedding frequency from the upstream cylinder. The probe was placed at the center plane of the test section at x/D = 2.5 and y/D = 1.0.

The power spectral density distributions of the streamwise velocity for a single square cylinder at Re = 5,300 and Re = 16,000 are shown in Fig. 23. The dominant peak frequency was f = 25.94 Hz for Re = 5,300 and f = 80.57 Hz for Re = 16,000.

The Strouhal number was defined by

$$St = \frac{fD}{U_\infty}, \tag{3}$$

where U_∞ is the freestream velocity, D is the width of the square cylinder, and f is the dominant peak frequency of the streamwise velocity. The Strouhal numbers at Re = 5,300 and Re = 16,000 were St = 0.134 and 0.138, respectively. Okajima [14] reported that St = 0.133 for $1.0 \times 10^3 < Re < 2.0 \times 10^4$ when the upstream turbulence intensity was less than 0.5%, while Chen and Liu [15] found that the Strouhal number changed from 0.125 to 0.138 over $2.0 \times 10^3 < Re < 2.1 \times 10^4$ when the upstream turbulence intensity was less than 0.5%. The variations in the Strouhal number for different spacings in our investigation are shown in Fig. 24. As the spacing between the two cylinders increased, the shedding frequency at the critical spacing s/D = 2.5 dropped to St = 0.114 and 0.112 for Re = 5,300 and Re = 16,000, respectively, and asymptotically approached the value for a single square cylinder.

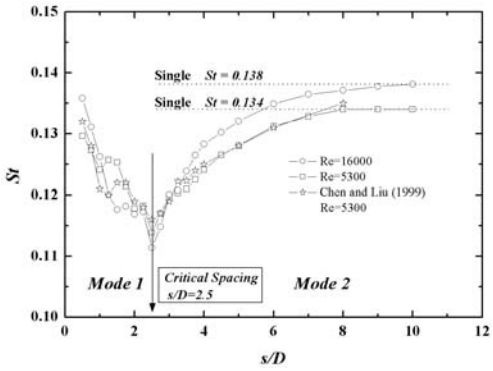

Fig. 24.Variation in the Strouhal number with the spacing.

4. Conclusions

The velocities, turbulence intensities, Reynolds shear stresses, and turbulent kinetic energies of the flow fields around two square cylinders in a tandem arrangement were investigated by using PIV. Our conclusions are as follows.

1) The flow characteristics can be divided into two different flow patterns separated by the critical spacing s/D = 2.5. The Mode 1 pattern had large recirculation regions between the two cylinders caused by the separated shear layer of the upstream cylinder that reattached on the lateral surface of the downstream cylinder. The Mode 2 pattern had separated shear layers at both the upstream and downstream cylinders.
2) The change in the Reynolds number from 5,300 to 16,000 had little effect on the streamwise velocity fields for the different spacings, whereas two completely different streamwise velocity patterns were identified. These were separated by the critical spacing s/D = 2.5. In particular, the maximum accelera-tion regions for the Mode 1 flow pattern were wider than those of the Mode 2 flow pattern.
3) The negative spanwise velocity that entered the gap between the two cylinders increased in proportion to the positive spanwise velocity that was separated from the upstream cylinder.
4) The streamwise turbulence intensity remained almost unchanged for Re = 5,300 and Re = 16,000. However, the spanwise turbulence intensity was affected by the two Reynolds numbers, despite the similar flow patterns.
5) In the region x/D = 1.0–2.5 and y/D = 0.5–1.0, the Reynolds shear stress distributions were greater and broader when Re = 16,000 compared to Re = 5,300. This was attributable to a momentum difference in the transport of the separated shear flow from the upstream cylinder to the gap between the two cylinders.
6) At Re = 5,300, the separated shear layers at both upstream corners of the upstream cylinder met at the front face of the downstream cylinder. However, at Re = 16,000, the separated shear layers met farther upstream near x/D = 2.5.
7) Since the spanwise velocity fluctuations were much larger than streamwise velocity fluctuations, the TKE characteristics along the centerline were similar to the spanwise turbulence intensity. At Re = 16,000, the maximum TKE observed near x/D = 0.3 was caused by the entrance of the surrounding fluids and their subsequent mixing.
8) As the spacing between the two cylinders increased, the shedding frequency at s/D = 2.5 dropped to St = 0.114 and 0.112 for Re = 5,300 and Re = 16,000, respectively, and asymptotically approached the value for a single square cylinder.

References

[1] H. Haniu, Y. Obata and H. Sakamoto, Fluctuating forces acting on two square prisms in a tandem arrangement, *J. Wind Eng & Ind. Aerodyn* 26 (1987) 85-103.

[2] H. Haniu and H. Sakamoto, Effect of free-stream turbulence on characteristics of fluctuating forces acting on two square prisms In tandem arrangement, *Transaction of ASME* 110 (1988) 140-146.

[3] Z. F. Gu, On interference between two circular cylinders at supercritical Reynolds number, *J. Wind Eng & Ind. Aerodyn* 62 (1996) 175-190.

[4] Z. F. Gu and T. F. Sun, Interference between wind loading on group of structures, *Wind Eng & 1nd. Aerodyn* 54/55 (1995) 213-225.

[5] H. Hangan and B. I. Vickery, Buffeting of two-dimensional bluff bodies, *Wind Eng & Ind Aerodyn* 82 (1999)173-187.

[6] H. Hangan, B. Havel and R. Martinuzzi, Buffeting for 2D and 3D sharp-edged bluff bodies, *Wind Eng & lnd. Aerodyn* 89 (2001) 1369-1381.

[7] J. M. Chen and C. H. Liu, Observations of hysteresis in flow around two square cylinders in a tandem arrangement, *Wind Eng & Ind. Aerodyn* 90 (2002) 1019-1050.

[8] B. Havel and R. 1. Martinuzzi, Vortex shedding from two surface-mounted cubes in tandem, *Heat & Fluids Flow* 25 (2004) 364-372.

[9] M. D. Mahbub, M. Moriya, H. Sakamoto and K. Takki, Suppression of fluid forces acting on two square prisms in a tandem arrangement by passive control of flow, *Fluids & Structures* 16(8) (2002) 1073-1092.

[10] R. J. Adrian, Particle-imaging techniques for experimental fluid mechanics, *Annual Review of Fluid Mech.* 23 (1991) 261-304.

[11] P. W. Bearman, On vortex shedding from a circular cylinder the critical Reynolds numbers regime, *J. Fluid Mech.* 37(3) (1969) 577-585.

[12] O. M. Criffn and S. E. Ramberg, Vortex shedding from a cylinder vibrating in line with and incident

uniform flow, *J. Fluid Mech.* 75(2) (1976) 257-271.
[13] J. R. Filler, P. L. Marston, and W. C. Mih, Response of the shear layers separating from a circular cylinder to small-amplitude rotational oscillations, *J. Fluid Mech.* 231 (1991) 481-499.
[14] A. Okajima, Strouhal numbers of rectangular cylinders, *J. Fluid Mech.* 123 (1982) 379-398.
[15] J.M. Chen and C.H. Liu, Vortex shedding and surface pressures on a square cylinder at incidence to a uniform air stream, *Heat & Fluids Flow* 20 (1999) 592-597.
[16] P. Bradshaw, An instruction to turbulence and its measurement, Pergamon Press, (1968).
[17] M. Arie and H. Rouse, Experiments on two-dimensional flow over a normal wall, *J. Fluid Mech.* 1 (Pt. 2), (1956) 129-141.